Transition Met Chem (2016) 41:235–248
DOI 10.1007/s11243-015-0015-2

Kinetic and mechanistic studies of cisplatin analogues bearing 2,2′-dipyridylalkylamine ligands

Grace Kinunda[1] · **Deogratius Jaganyi**[1]

Received: 27 November 2015 / Accepted: 1 December 2015 / Published online: 17 December 2015
© Springer International Publishing Switzerland 2015

Abstract A series of mononuclear Pt(II) complexes of the type diaqua(2,2′-dipyridylalkylamine)platinum(II) (where the alkyl group = methyl, ethyl, propyl, butyl or hexyl) were synthesized to investigate their nucleophilic substitution behaviour and the influence of the alkyl chain bonded to the tertiary nitrogen atom joining the two pyridine rings on the reactivity of the chosen complexes. The trend in rate constant shows that introduction of the σ-donating alkyl chain on the tertiary nitrogen joining the two pyridine moieties reduces the π-acceptor ability of the *cis* coordinated pyridine rings resulting in a less reactive Pt(II) centre which causes a decrease in the reaction rate. This is well supported by data from DFT calculations. It is also evident that the alkyl chain also introduces a steric effect which blocks the approach of the nucleophile to the Pt(II) centre. The boat-like structure of the six-membered chelate ring also contributes to the steric effect. The study has also shown that two substitution processes going through an associative mode of activation are observed. The first is the simultaneous substitution of the two aqua ligands, and the second is due to the dechelation of the ligand, an indication of possible disintegration of the complex if used as a drug.

Electronic supplementary material The online version of this article (doi:10.1007/s11243-015-0015-2) contains supplementary material, which is available to authorized users.

✉ Deogratius Jaganyi
jaganyi@ukzn.ac.za

[1] School of Chemistry and Physics, University of KwaZulu-Natal, Scottsville 3209, South Africa

Introduction

The kinetic study on the interaction of various platinum(II) complexes with nucleophiles often reveals important chemical behaviour of these compounds in the area of chemotherapy. This work reports the kinetics of Pt(II) complexes featuring 2,2′-dipyridylamine (dpa). 2,2′-Dipyridylamine is an aromatic amine which behaves as a neutral or monoanionic ligand. The NH group is usually not involved in coordination because of geometrical constraints, and the two pyridine rings are flexible in their coordination to metal centres, leading to different coordination modes such as monodentate, chelating bidentate and bridging tridentate [1–6]. It is well established that upon coordination with a metal centre, dpa forms a six-membered chelate ring with the pyridyl rings adopting either nearly co-planar or inclined pyridyl ring planes. This property of dpa and its derivatives affects either the electronic or stereo chemical properties of the systems and has been observed in a number of metal complexes [7].

To date, platinum(II) complexes of 2,2′-dipyridylamine (dpa) have received increasing attention and have been investigated due to their potential use as anticancer agents owing to their structural similarity to cisplatin [8–10]. Reactions with model nucleobases and cytotoxicity of mononuclear complexes with a 2,2′-dipyridylamine ligand system have been extensively studied [11–15]. Results show that the 2,2′-dipyridylamine unit provides a favourable structural feature for an unhindered DNA–complex interaction [16] leading to significant cytostatic activities in the range of cisplatin in several tumour cell lines [17, 18].

Substitution reactions on Pt(II) complexes with N–N/N–S bidentate ligands such as ethylenediamine (en), bipyridine (bpy), aminomethylpyridine (amp) and thiomethylpyridine (mtp) have been investigated [19–23]. Results show that the

lability of the leaving groups depends on the electronic and steric effects of the bidentate ligand. For example, substitution reactions of the complexes *cis*-$[Pt(NH_3)_2Cl_2]$, $[Pt(SMC)Cl_2]^-$, $[Pt(en)Cl_2]$ and $[Pt(dach)Cl_2]$ (where SMC = S-methyl-L-cysteine, en = ethylenediamine and dach = 1,2-diaminocyclohexane) follow the trend $[Pt(SMC)Cl_2]^- >$ *cis*-$[Pt(NH_3)_2Cl_2] > [Pt(en)Cl_2] > [Pt(dach)Cl_2]$ [19]. The high reactivity of $[Pt(SMC)Cl_2]^-$ was attributed to the strong *trans* labilization effect of coordinated sulphur donor, because the strong σ-donating effect of sulphur leads to elongation of the Pt–Cl bond in the *trans* position, therefore making it more labile. Similar results on the *trans* labilizing effect of sulphur were also reported by van Eldik et al. [21, 23]. The reactivity of the complexes *cis*-$[Pt(NH_3)_2Cl_2]$, $[Pt(en)Cl_2]$, $[Pt(dach)Cl_2]$ depends on the steric effects. $[Pt(dach)Cl_2]$ is reported to be the most sterically congested complex because of the cyclohexane ring which also imparts a positive inductive effect to the metal centre and making it less electrophilic [19, 20]. In a related study where the π-acceptor groups of the bidentate ligand were varied, it was found that the electrophilicity on the Pt(II) centre increased due to the electron-withdrawing properties of the π-acceptor groups, which results in increasing reaction rates for nucleophilic substitution reactions especially when two pyridine rings are adjacent to each other [22].

To extend the understanding on the effect of π-acceptors on the thermodynamic and kinetic properties of Pt(II) complexes, a series of five Pt(II) complexes with dpa ligands (Scheme 1), namely diaqua(2,2′-dipyridylmethylamine)-platinum(II) (**Ptdpma**), diaqua(2,2′-dipyridylethylamine) platinum(II) (**Ptdpea**), diaqua(2,2′-dipyridylpropylamine)-platinum(II) (**Ptdppa**), diaqua(2,2′-dipyridylbutylamine) platinum(II) (**Ptdpba**), and diaqua(2,2′-dipyridylhexylamine) platinum(II) (**Ptdpha**), were therefore chosen and their kinetic behaviour investigated so as to provide an understanding of their interactions with sulphur donor nucleophiles. The ligand 2,2′-dipyridylamine was altered by incorporating an alkyl group of variable chain length on the tertiary nitrogen of the bidentate chelate. This endowed surfactant properties to the resulting Pt(II) complexes which is known to improve diffusion through cell membranes, hence facilitating their entrance into the cell compared to cisplatin [24]. For comparison purposes, kinetic data for Pt(bpy) (where bpy = N,N′-bipyridine) which also contains two pyridine rings in the bidentate chelate were included. The two pyridine rings of Pt(dpa) complexes are more flexible in coordination compared to Pt(bpy). This is expected to affect the electronic properties of the Pt(II) centre and hence the substitution reactions. The thiourea nucleophiles were chosen because of their good solubility, neutral character, different nucleophilicity, steric hindrance, binding properties and biological relevance [25, 26]. In addition, thiourea is a very useful nucleophile since it combines the properties of thiolates (σ-donor) and thioethers (σ-donor and π-acceptor) [25, 27, 28].

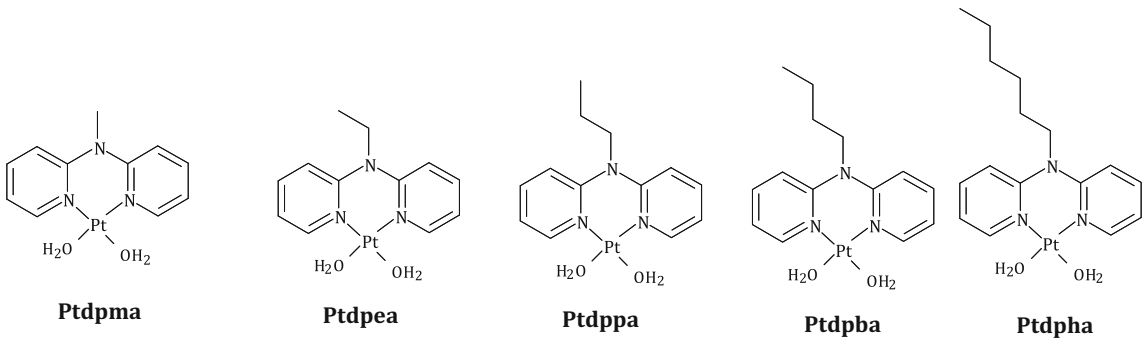
Experimental

Chemicals

Potassium tetrachloroplatinate, K_2PtCl_4 (99 %), was purchased from Strem Chemicals. The nucleophiles thiourea (TU, 99 %), 1,3-dimethyl-2-thiourea (DMTU, 99 %), 1,1,3,3-tetramethyl-2-thiourea (TMTU, 98 %) and reagents methyl iodide (99 %), 1-bromoethane (99 %), 1-bromopropane (97 %), 1-bromobutane (98 %), 1-bromohexane and 2,2′-dipyridylamine (97 %) were obtained from Aldrich and used without further purification. $AgClO_4$ (99.99 %, Aldrich) was stored under nitrogen and used as supplied. Ultrapure water (PureLab Systems) was used in all experiments. All other reagents used were of analytical grade quality and were used without further purification.

Synthesis of the ligands

The ligands, namely (2,2′-dipyridyl)methylamine (**dpma**), (2,2′-dipyridyl)ethylamine (**dpea**), (2,2′-dipyridyl)-1-propylamine (**dppa**), (2,2′-dipyridyl)-1-butylamine (**dpba**), and



Scheme 1 Structures of the complexes investigated

(2,2′-dipyridyl)-1-hexylamine (**dpha**), were synthesized using the same procedure [15] starting from 2,2′-dipyridylamine and their respective bromo alkyl halides. For **dpma**, methyl iodide was used as a precursor.

To a suspension of potassium hydroxide (1.3 g, 0.02 mol) in 15 mL of DMSO, 2,2′-dipyridylamine (0.0855 g, 0.5 mmol) was added. The mixture was stirred at room temperature for 45 min after which the respective alkyl halide (0.5 mmol) was added. After stirring at room temperature for a further period of 60 min, 20 mL of water was added. The solution was extracted with diethyl ether (30 mL), and the organic extracts dried over $MgSO_4$. The solvent was removed in vacuo to yield the desired ligand. All ligands were characterized by NMR spectroscopy and LC–MS and used for complex formation without further purification.

dpma Brown oil, yield 49.3 mg (53.3 %). ^{1}H NMR ($CDCl_3$, 400 MHz): $\delta = 8.23$ (ddd, 2H), 7.44 (ddd, 2H), 7.06 (td, 2H), 6.76 (dd, 2H), 3.53 (s, 3H). ^{13}C NMR ($CDCl_3$, 400 MHz): 157.6, 148.1, 137.1, 116.9, 114.4 and 36.1. TOF MS ES$^+$: m/z $[M + H]^+ = 186.01$.

dpea Yellow oil, yield 55.4 mg (55.7 %). ^{1}H NMR ($CDCl_3$, 400 MHz): $\delta = 8.10$ (dd, 2H), 7.31 (dddd, 2H), 6.86 (brd, 2H), 6.64 (dddd, 2H), 4.00 (t, 2H), 1.03(t,3H). ^{13}C NMR ($CDCl_3$, 400 MHz): 157.0, 148.1, 137.0, 116.8, 114.6, 39.2 and 13.3. TOF MS ES$^+$: m/z $[M + H]^+ = 200.12$.

dppa Brown oil, yield 54.5 mg (51.2 %). ^{1}H NMR ($CDCl_3$, 400 MHz): $\delta = 8.15$ (dddd, 2H), 7.36 (dddd, 2H), 6.91 (dddd, 2H), 6.68 (dddd, 2H), 3.96 (t, 2H), 1.55 (m, 2H), 0.76 (t, 3H). ^{13}C NMR ($CDCl_3$, 400 MHz): 157.4, 148.1, 137.0, 116.7, 114.6, 49.81, 21.3 and 36.1. TOF MS ES$^+$: m/z $[M + H]^+ = 214.13$.

dpba Brown oil, yield 60.5 mg (53.3 %). ^{1}H NMR ($CDCl_3$, 400 MHz): $\delta = 7.93$ (dddd, 2H), 7.15 (dddd, 2H), 6.70 (dddd, 2H), 6.48 (dddd, 2H), 3.78 (t, 2H), 1.28 (m, 2H), 0.98 (m, 2H), 0.53 (t, 3H). ^{13}C NMR ($CDCl_3$, 400 MHz): 147.8, 136.9, 115.9, 114.7, 47.7, 30.0, 19.9 and 13.7. TOF MS ES$^+$: m/z $[M + H]^+ = 228.15$.

dpha Brown oil, yield 69.6 mg (54.6 %). ^{1}H NMR ($CDCl_3$, 400 MHz): $\delta = 7.84$ (dddd, 2H), 7.07 (dddd, 2H), 6.62 (brd, 2H), 6.39 (dddd, 2H), 3.68 (t, 2H), 1.20 (m, 2H), 0.83 (m, 6H), 0.40 (t, 3H). ^{13}C NMR ($CDCl_3$, 400 MHz): 157.0, 147.8, 136.8, 115.7, 114.5, 47.8, 30.5, 27.8, 25.9, 22.2 and 13.7. TOF MS ES$^+$: m/z $[M + H]^+ = 256.18$.

Synthesis of the complexes

The complexes **Ptdpma**, **Ptdpea**, **Ptdppa**, **Ptdpba** and **Ptdpha** were synthesized from their respective ligands according to a literature method [10]. To a stirred red solution of 0.2075 g (0.5 mmol) K_2PtCl_4 dissolved in 25 mL of water, the corresponding ligand (0.5 mmol) dissolved in a small amount of water was added. The reaction mixture was stirred overnight at 50 °C. The resulting yellow precipitate was collected, washed with water, ethanol, methanol and diethyl ether, and dried in vacuum. The purity of the complexes was confirmed by NMR, LC–MS and elemental analysis.

Ptdpma Yield 132.3 mg, (52.3 %). ^{1}H NMR (DMSO-d_6, 400 MHz) $\delta = 8.84$ (ddd, 2H), 8.11 (ddd, 2H), 7.50 (td, 2H), 7.28 (dd, 2H), 3.66 (s, 3H). ^{13}C NMR (DMSO-d_6, 400 MHz): 153.5, 151.6, 141.5, 121.2, 115.3 and 40.9. *Anal. % calcd*. for $C_{11}H_{11}Cl_2N_3Pt$: C 29.27, H 2.44, N 9.31. *Found*: C 28.85, H 2.50, N 8.87. TOF MS ES$^+$: m/z $[M + Na]^+ = 473.99$.

Ptdpea Yield 94.4 mg, (40.6 %). ^{1}H NMR (DMSO-d_6, 400 MHz): $\delta = 8.10$ (dd, 2H), 7.31 (dddd, 2H), 6.86 (brd, 2H), 6.64 (dddd, 2H), 4.00 (t, 2H), 1.03(t,3H). ^{13}C NMR (DMSO-d_6, 400 MHz): 153.3, 151.8, 141.5, 121.6, 116.9, 45.1 and 13.7. *Anal. % calcd*. for $C_{12}H_{13}Cl_2N_3Pt$: C 30.97, H2.79, N 9.03. *Found*: C 30.71, H 2.82, N 8.74. TOF MS ES$^+$: m/z $[M + Na]^+ = 488.00$.

Ptdppa Yield 136.7 mg, (57.1 %). ^{1}H NMR (DMSO-d_6, 400 MHz): $\delta = 8.81$ (dd, 2H), 8.09 (dddd, 2H), 7.54 (dddd, 2H), 7.29 (dddd, 2H), 4.09 (t, 2H), 1.67 (m, 2H), 1.09 (t, 3H). ^{13}C NMR (DMSO-d_6, 400 MHz): 153.3, 151.7, 141.4, 121.6, 117.0, 51.9, 20.8 and 11.6. *Anal. % calcd*. for $C_{13}H_{15}Cl_2N_3Pt$: C 32.56, H 3.13, N 8.76. *Found*: C32.67, H 3.15, N 8.40. TOF MS ES$^+$: m/z $[M + Na]^+ = 502.02$.

Ptdpba Yield 256.3 mg, (57.4 %). ^{1}H NMR (DMSO-d_6, 400 MHz): $\delta = 8.81$ (dd, 2H), 8.09 (dddd, 2H), 7.55 (d, 2H), 7.28 (dddd, 2H), 4.11 (t, 2H), 1.64 (m, 4H), 0.90 (t, 3H). ^{13}C NMR (DMSO-d_6, 400 MHz): 153.3, 151.7, 151.4, 121.6, 116.9, 50.3, 29.6, 19.7 and 14.0. *Anal. % calcd*. for $C_{14}H_{17}Cl_2N_3Pt$: C 34.07, H 3.45, N 8.52. *Found*: C 34.37, H 3.47, N 8.51. TOF MS ES$^+$: m/z $[M + Na]^+ = 516.03$.

Ptdpha Yield 108.6 mg, (41.7 %). ^{1}H NMR (DMSO-d_6, 400 MHz): $\delta = 7.84$ (dddd, 2H), 7.07 (dddd, 2H), 6.62 (brd, 2H), 6.39 (dddd, 2H), 3.68 (t, 2H), 1.20 (m, 2H), 0.83 (m, 6H), 0.40 (t, 3H). ^{13}C NMR (DMSO-d_6, 400 MHz): 153.3, 151.7, 141.4, 121.6, 116.9, 50.3, 31.1, 27.3, 26.5, 26.2 and 26.0. *Anal. % calcd*. for $C_{16}H_{21}Cl_2N_3Pt$: C 36.85, H 4.03, N 8.06. *Found*: C 37.14, H 4.03, N 7.59. TOF MS ES$^+$: m/z $[M + Na]^+ = 544.06$.

Preparation of diaqua Pt(II) complexes

Solutions of the aqua complexes were prepared by suspending an accurately weighed amount of the chloro

complex in 0.1 M $HClO_4$ and adding a stoichiometric amount of $AgClO_4$ (1.98 equiv) with respect to chloro complex. The mixture was then stirred in the dark at 50 °C for 24 h. The white precipitate of silver chloride which formed was removed with a 0.45-μm nylon membrane filter using a Millipore filtration unit. The clear, colourless filtrate was then made to the required concentration in a volumetric flask using a solution of 0.1 M $HClO_4$. The use of the acidic solution at pH 1 was necessary to ensure that only the aqua complex, and not a mixture of the aqua and hydroxo complexes, was present in solution once the metathesis reaction was complete, and also, to ensure a constant ionic strength of 0.1 M. This solution was used in the titration with NaOH solution to determine the pK_a of the complexes, whilst for kinetic investigations, the pH of the solution was maintained at 2 based on the pK_a study and the ionic strength was maintained at 0.1 M using $NaClO_4$.

Instrumentation and measurements

^{1}H, ^{13}C and ^{195}Pt spectra were recorded on a Bruker Avance III 500 or Bruker Avance III 400 at frequencies of 500 or 400 MHz (1H) and 125 MHz/100 MHz using either a 5-mm BBOZ probe or a 5-mm TBIZ probe. All proton and carbon chemical shifts are reported relative to the relevant solvent signals at 30 °C unless stated otherwise. Elemental compositions of the ligands and complexes were obtained on a Thermo Scientific Flash 2000. The pH of the aqueous solutions of the complexes was measured using a Jenway 4330 Conductivity/pH meter equipped with a 4.5-μm-diameter glass electrode. The electrode was calibrated at 25 °C using standard buffer solutions of pH 4.0, 7.0 and 10.0 (Merck). The electrolyte of pH electrode was replaced with 3.0 M NaCl to prevent the precipitation of $KClO_4$ during pH measurement. The mass spectral data of the ligands and complexes were acquired on a Waters Micromass LCT Premier spectrometer. Kinetic studies for fast reactions were monitored using an Applied Photophysics SX 20 stopped-flow spectrophotometer coupled to an online data acquisition system. Slow reactions were monitored using a Varian UV–visible Cary 100 spectrophotometer. The temperature of these instruments was controlled throughout all kinetic experiments to ±0.02 °C. pK_a and kinetic traces were graphically analysed using the software package Origin 7.5® [29].

pK_a determination

In order to avoid formation of hydroxo species during kinetic studies, it was important to determine the pH range within which the complexes exist in their aqua form. The measured pK_a data are helpful in explaining the substitution lability of the aqua ligands in the metal complex as the p*K*a values of coordinated water serve as an experimental indicator for the electron density around the metal centre. The low pK_a values are associated with the most electrophilic and reactive Pt(II) centre and vice versa [19–23].

To determine pK_a values, a solution of the complex of known concentration was spectrophotometrically titrated with NaOH within the pH range of 1–10 at 25 °C. To avoid dilution effects due to the addition of the titrant, a large volume (150 mL) of the complex was used for the titration. To avoid adding a large volume of NaOH to effect the change in pH within the pH range of 1–3, small granules of crushed NaOH pellets were added to the solution. Between a pH range of 4–10, various concentrations of NaOH solutions were used, making sure that there was an even distribution of the UV–Vis spectra. To avoid contamination of the complex solution by chloride ions leaching from the pH electrode, it was necessary to take 0.6 mL aliquots from the complex solution, which was then transferred into narrow vials for the pH measurements. These were then discarded after each measurement. The reversibility of the titration was also tested using aqueous solutions of perchloric acid.

Kinetic measurements

All kinetic measurements were taken under *pseudo*-first-order conditions by making sure that the concentration of the nucleophile was at least 20-fold in excess to the concentration of Pt(II) complexes. This was to ensure that the reaction goes to completion. All the substitution reactions involving aqua complexes were studied at pH 2. Concentration dependence study of the complexes was performed at 25 °C. Reported rate constants in Table 4 represent an average value of at least three to five independent kinetic runs for each set of experimental conditions on UV–visible and stopped-flow spectrophotometers, respectively. The activation parameters, $\Delta H^{\#}$ and $\Delta S^{\#}$, were obtained by studying the temperature dependence of the rate constant in the temperature range of 15–35 °C at an interval of 5 °C with the nucleophile concentration held constant at 80 times the concentration of the metal complex.

Computational analysis

Density functional theoretical (DFT) calculations were performed with the Gaussian 09 program suite [30]. Geometrical optimizations were carried out at B3LYP/LanL2DZ level of theory. B3LYP refers to a three-parameter functional hybrid exchange of Becke [31] with functional correlation gradient of Lee et al. [32, 33], whilst LanL2DZ refers to Los Alamos National Laboratory 2 Double ζ [34] basis set. The

singlet states were used due to low electronic spin of Pt(II) complexes. The aqua complexes were each modelled at +2 with respect to their total charges.

Results

Acidity of the aqua complexes

The acidities of the coordinated diaqua ligands on the Pt(II) complexes were determined through spectrophotometric titration. A typical plot of the UV–visible spectra obtained during the course of the titration of the complex **Ptdpba** with NaOH is shown in Fig. 1. Inset in the figure is the plot of absorbance versus pH at 290 nm for the **Ptdpba**. When the data points of the plot of absorbance versus pH were fitted to a standard sigmoid equation using Origin 7.5® [29], it revealed that two dissociation steps were involved. This was observed for each of the investigated complexes. The overall process can therefore be presented by the equilibrium reaction given in Scheme 2. The pK_a values obtained are summarized in Table 1 and as stated before for comparison purposes included in the table is the pK_a value of **Pt(bpy)**. The results show that changing the length of the alkyl group attached to the spacing tertiary nitrogen of the bidentate chelate has insignificant influence on the deprotonation of the aqua molecules as the pK_a values are similar in magnitude, true for both deprotonation steps.

It is also observed that deprotonation of the second coordinated water molecule to the dihydroxo species occurs at higher pH values than in the first step in all the five complexes. This results from a reduction of the overall charge to +1 after deprotonation of one coordinated water ligand. Hence, the Pt(II) centre of the aqua/hydroxo species is less electrophilic compared to the diaqua complex [35–38], leading to higher pK_{a2} values. The lower pK_a value of **Pt(bpy)** is ascribed to rigid and planar π-acceptor pyridine moieties *cis* to the aqua ligands which help to stabilize the electron density of the hydroxo ligands formed, making the complex more electrophilic and acidic.

Computational studies

The geometry-optimized structures and the mapping of frontier molecular orbitals are presented in Table 2. The bidentate dpa ligand coordinates the metal centres via its two nitrogen donor atoms forming a six-membered chelating ring which exists in a boat conformation due to high flexibility of the nitrogen linker between the coordinated pyridines. Two aqua ligands complete the coordination spheres, resulting in a square planar geometry around the metal centre. The two heterocyclic rings of dpa form a dihedral angle in a range of 38° to 42°. The basal angle around the Pt centre of all complexes with respect to the *cis* pyridine rings lies between 113° and 119° (Fig. 2 and Figure SI 27). The calculated bond lengths and angles

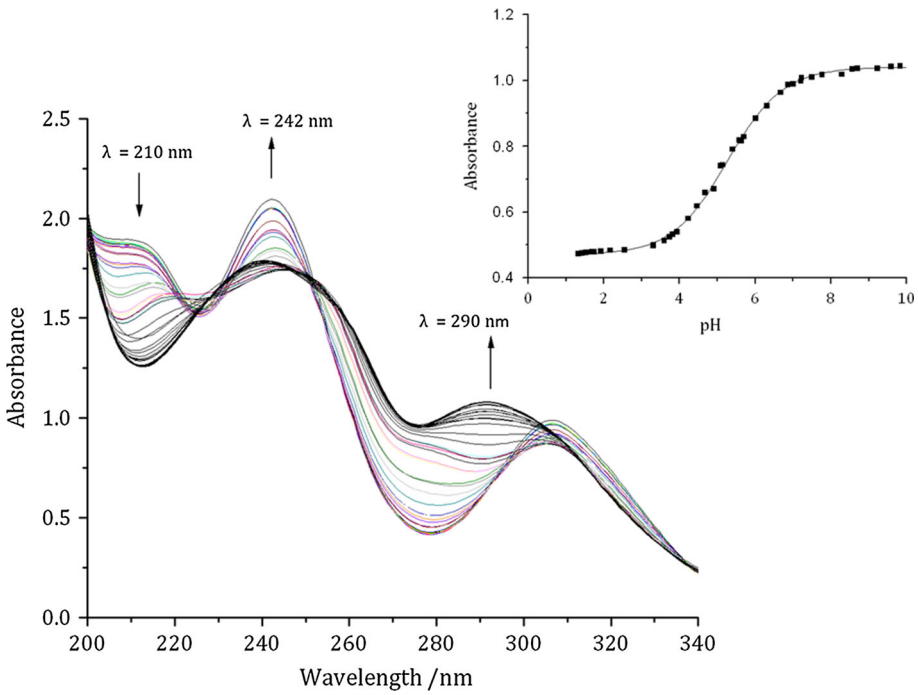
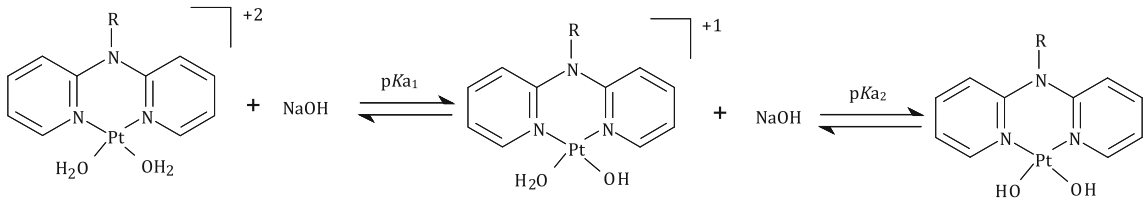


Fig. 1 UV–visible spectra of the titration of **Ptdpba** with NaOH (pH range 1–10). *Inset* Plot of absorbance versus pH at 290 nm for the **Ptdpba**



Scheme 2 Schematic presentation of the acid dissociation equilibria of the investigated complexes

Table 1 Observed pK_a values for the deprotonation of Pt-bound aqua ligands for each of the mononuclear Pt(II) complexes investigated

Complex	Ptdpma	Ptdpea	Ptdppa	Ptdpba	Ptdpha	Pt(bpy)
pK_{a1}	5.24 ± 0.07	5.27 ± 0.02	5.31 ± 0.03	5.36 ± 0.08	5.45 ± 0.12	4.80*
pK_{a2}	6.19 ± 0.04	6.29 ± 0.07	6.29 ± 0.02	6.31 ± 0.06	6.35 ± 0.11	6.32*

* pK_a values extracted from Ref. [22]

(Table 3) fit well with the values given in the literature for chloro complexes of Pt(II) and Pd(II) [14].

Mappings of the frontier orbitals indicate that for all investigated complexes, the HOMOs are localized mainly on the platinum metal with significant contribution from the pyridine rings and the $(CH_2)_n$ units of the alkyl chain. The LUMOs of these complexes are symmetrically delocalized on the Pt atom, pyridine nitrogens and aqua groups. Because of the location of HOMO and LUMO, an electron-donating effect would be expected to increase electron density on the complex as a whole, raise the HOMO energy and destabilize the LUMO. The individual energy levels of the HOMO and LUMO increase with the length of the aliphatic chain from **Ptdpma** to **Ptdpha**. This trend can be explained by the increase in σ-donicity of the alkyl chain to the pyridyl side arms with increasing length of the alkyl chain. The literature shows that the presence of electron-donating groups in a system increases the energy of the molecular orbitals [39–42].

Included in Table 3 is global chemical reactivity descriptor for electrophilicity indices of the complexes calculated using a literature method [43]. Electrophilicity values of the complexes (Table 3) follow the trend **Ptdpha** < **Ptdpba** < **Ptdppa** < **Ptdpea** < **Ptdpma**. Among the complexes, **Ptdpha** is the weakest electrophile whilst **Ptdpma** is the strongest electrophile. It is worth noting that the NBO charges of the Pt atom are of the same magnitude, so the influence of the σ-donor ability of the alkyl chain to the metal centre is minimal.

Kinetic measurements

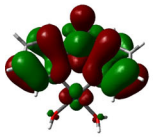
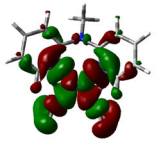
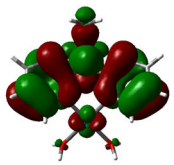
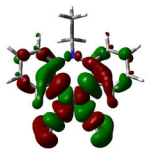
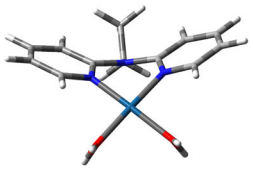
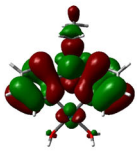
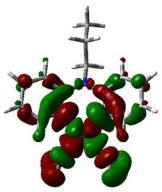
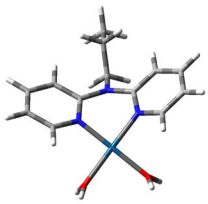
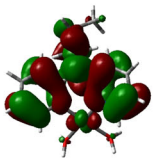
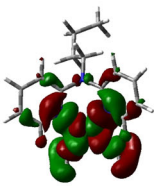
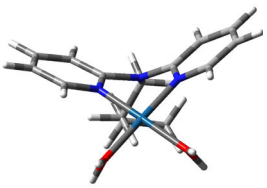
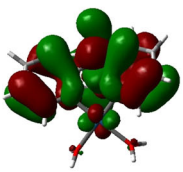
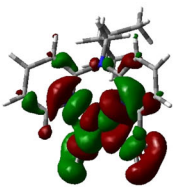
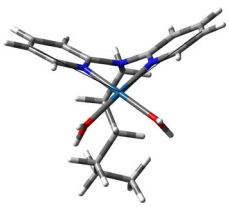
Spectral changes resulting from mixing of the Pt(II) complex and nucleophile solutions were recorded over the wavelength range 200–600 nm to establish a suitable wavelength at which kinetic measurements could be performed. The selected wavelengths are summarized in Table SI 1. The substitution reactions of the aqua complexes by a series of neutral nucleophiles, viz. TU, DMTU and TMTU, were investigated as a function of concentration and temperature. All the reactions showed two independent substitution steps (Scheme 3). Whilst the first step could be followed by stopped flow, the second step was too slow and was followed by conventional UV–visible spectroscopy for only the two less sterically hindered nucleophiles TU and DMTU. The reactions with TMTU were too slow, taking more than 5 days to go to completion.

The first substitution step was initiated by mixing equal volumes of a solution of the Pt(II) complex with a solution of the nucleophile directly in the stopped-flow instrument set at a selected wavelength. An example of the kinetic trace is shown in Fig. 3. Typical UV–visible spectra obtained for the second substitution step are shown in Fig. 4 and inset in Fig. 4 is its corresponding kinetic trace at 315 nm.

In both steps, the kinetic traces for the ligand substitutions gave excellent fits to a single exponential function to generate the *pseudo*-first-order rate constants, $k_{obs1/2}$, at specific nucleophile concentrations and temperature. The second-order rate constants, k_1 and k_2, of the reactions were obtained from the linear regression of the plot of $k_{obs1/2}$ versus nucleophile concentration using Origin 7.5® [29].

Representative plots for each of the investigated nucleophiles show a linear dependence on the concentration of the incoming nucleophile and are shown in Fig. 5 (also Figures SI 19-21 and SI 25). The linear regression plots did

Table 2 Geometry-optimized structures and DFT-calculated B3LYP/LanL2DZ HOMOs sand LUMOs for the investigated complexes

Complex	HOMO	LUMO	Planarity
Ptdpma			
Ptdpea			
Ptdppa			
Ptdpba			
Ptdpha			

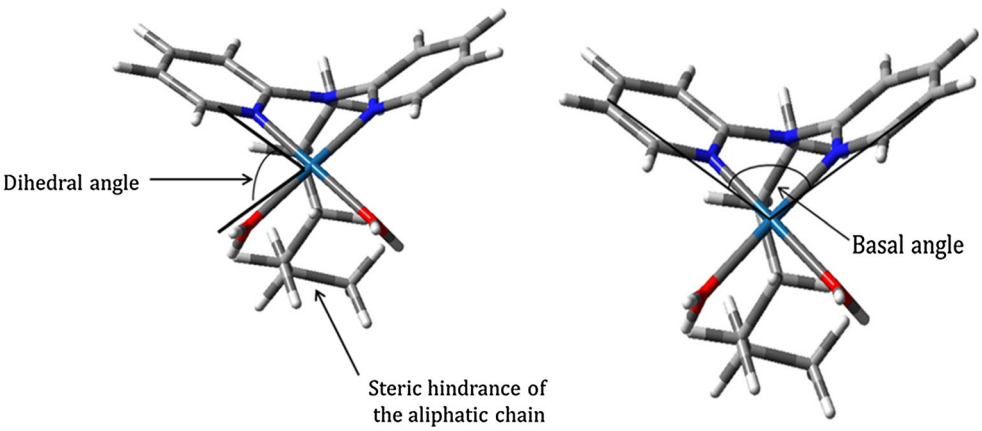
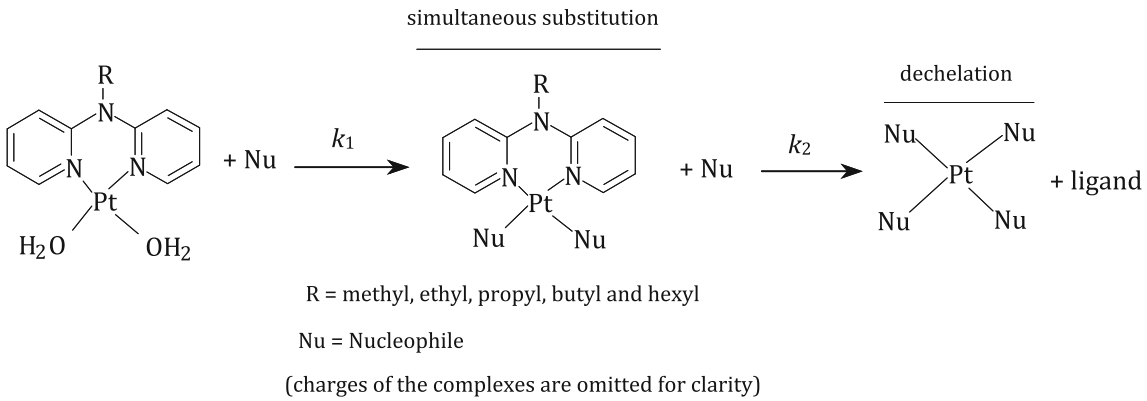


Fig. 2 DFT-optimized structures of **Ptdpha** showing dihedral angle, steric hindrance of the aliphatic chain and basal angle of the boat-conformed pyridine rings

Table 3 DFT-calculated parameters for the investigated Pt(II) complexes

	Ptdpma	Ptdpea	Ptdppa	Ptdpba	Ptdpha
HOMO–LUMO energy					
LUMO/eV	−9.094	−8.901	−8.862	−8.833	−8.794
HOMO/eV	−12.913	−12.872	−12.793	−12.785	−12.723
ΔE/eV	3.819	3.971	3.931	3.952	3.929
Reactivity descriptors					
Electrophilicity index (ω)	31.704	29.845	29.823	29.564	29.459
NBO charges					
Pt	0.762	0.759	0.759	0.756	0.757
$N_{1/2}$	−0.520	−0.523	−0.523	−0.525	−0.528
N_3	−0.489	−0.495	−0.491	−0.507	−0.511
Dipole moment (debye)	2.678	3.648	4.803	5.209	6.469
Bond length (Å)					
Pt–O_1	2.125 (46)	2.128 (58)	2.128 (93)	2.126 (98)	2.125 (46)
Pt–O_2	2.125 (62)	2.128 (66)	2.128 (90)	2.126 (23)	2.125 (62)
Bond angles (°)					
Dihedral	39.94	38.53	38.13	41.26	42.10
N_2–Pt–O_1	177.961	175.834	177.950	178.215	177.904
N_1–Pt–O_2	177.949	177.812	177.953	178.514	178.605
N_1–Pt–N_2	87.973	87.717	87.763	87.722	87.651
O_1–Pt–O_2	87.506	86.878	86.835	87.623	87.396

R = alkyl group



Scheme 3 Proposed reaction scheme of aqua substitution from the investigated Pt(II) complexes and the thiourea nucleophiles at pH 2.0

not have nonzero intercepts, which suggests that the mechanistic pathway is independent of the solvent effect. The proposed equations for the two substitution steps can be represented by Eq. 1.

$$k_{\text{obs}1/2} = k_{1/2}[\text{Nu}] \quad (1)$$

The activation parameters: the enthalpy of activation, $\Delta H^{\#}$, and entropy of activation, $\Delta S^{\#}$, of each substitution step were determined by studying the temperature dependence of the rate constants, k_1 and k_2, at a fixed nucleophile concentration. Typical plots are shown in Fig. 6 (also Figures SI 22-24), and the corresponding values were calculated using the Eyring equation [44, 45]. A summary of rate constants and activation parameters for the first and second substitution steps is given in Table 4.

To further understand the kinetics of the second and slower step of the reaction, the ligand substitutions of **Ptdppa–Cl** were followed using ^{1}H and ^{195}Pt NMR. An array of the ^{1}H NMR spectra (showing only the aromatic resonances) for the reaction between **Ptdppa–Cl** and excess

TU (six equivalents) is shown in Fig. 7. The pyridyl protons were chosen to monitor the progress of the reaction as they are in close proximity to the N-donor atom bonded to the metal centre. The numbering scheme employed for the pyridyl protons is shown in the structure of the **Ptdppa–Cl_2** complex in Scheme 4.

The resonances of the unreacted **Ptdppa–Cl_2** protons labelled H_5, H_4, H_3 and H_2 appear at $\delta = 8.82$, 8.10, 7.55 and 7.28 ppm, respectively, with the ^{195}Pt NMR peak at $\delta = -2178.9$ ppm (Fig. 8). The ^{1}H and ^{195}Pt NMR spectra show that within the timescale of the reaction only two main products had been formed. These are identified as uncoordinated **dppa** ligand with its aromatic protons appearing at $\delta = 8.29$, 7.62, 7.11 and 6.93 ppm for $H_{5'}$, $H_{4'}$, $H_{3'}$ and $H_{2'}$, respectively, and the ^{195}Pt peak at $\delta = -3914.2$ ppm corresponding to $Pt(TU)_4$. No intermediate peaks were observed in the ^{195}Pt NMR spectra during the course of reaction; thus, the coordinated aqua ligands are simultaneously substituted from the Pt(II) centre in the first step. The disappearance of the original ^{1}H and ^{195}Pt NMR peaks of **Ptdppa–Cl_2** and the appearance of the ^{195}Pt NMR peak at $\delta = 3914.2$ ppm corresponding to $Pt(TU)_4$ all support the proposed reaction given in Scheme 3.

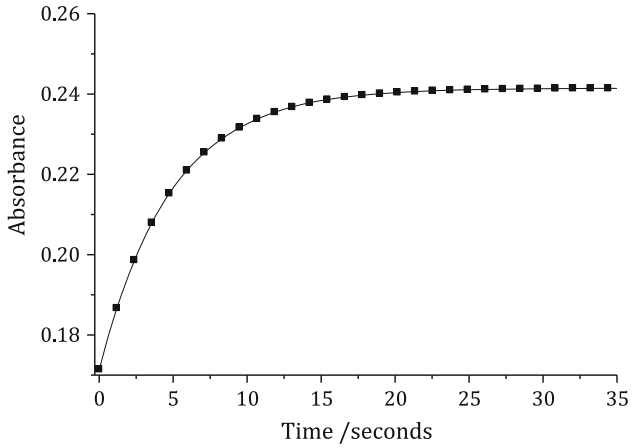


Fig. 3 A typical kinetic trace for two-step reaction between **Ptdppa** (0.25 mM) and TU (20 mM) recorded at 290 nm, $T = 298$ K, pH 2.0, $I = 0.1$ M ($NaClO_4$) on the stopped-flow spectrophotometer

Discussion

As stated before, all substitution reactions were characterized by two steps. The first step involves simultaneous displacement of the aqua ligands, and the second step involved dechelation of the dipyridylamine ligand following the coordination of further thiourea nucleophiles to the Pt(II) centre. This conclusion was arrived at after monitoring the reaction between **Ptdppa–Cl_2** and TU (excess) by ^{1}H and ^{195}Pt NMR spectroscopy.

It is well known from the literature that ^{195}Pt NMR is effective in identifying the species in solution. The ^{195}Pt chemical shifts are influenced by all the ligands in the coordination sphere of the Pt atom and are highly sensitive to the nature of the binding atoms [46, 47]. The σ-bond between the ligand and the metal (L→M) reduces the electron density on the ligand and increases it on the Pt atom. If there is a back-donation of π electrons (M→L), the electron density is then reduced on the Pt atom and is

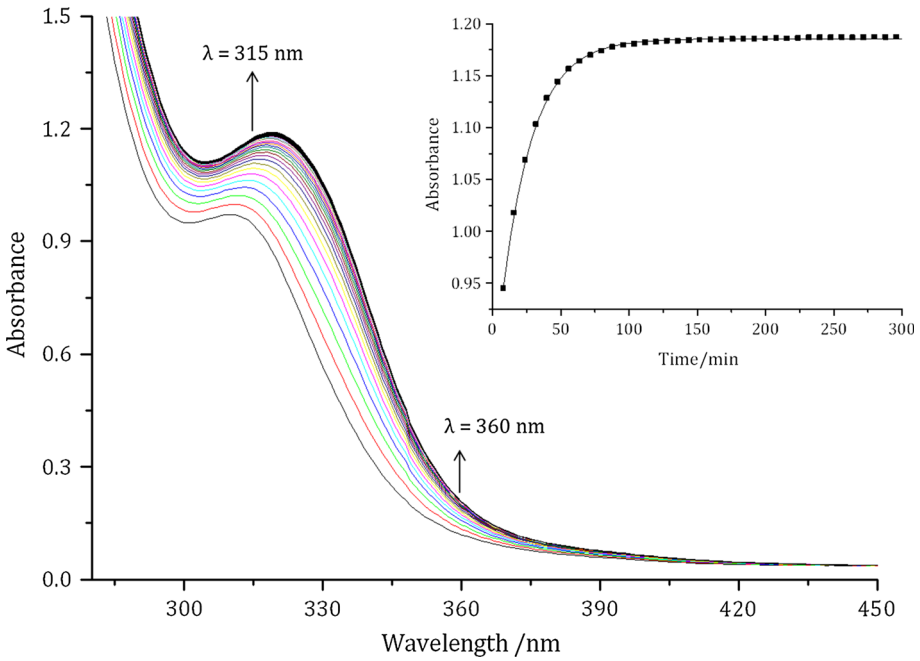


Fig. 4 UV–visible spectra recorded during the reaction of 0.25 mM **Ptdppa** with 30 mM thiourea at 25 °C and pH 2 ($I = 0.1$ M, $NaClO_4$). *Inset* Kinetic trace recorded at 315 nm

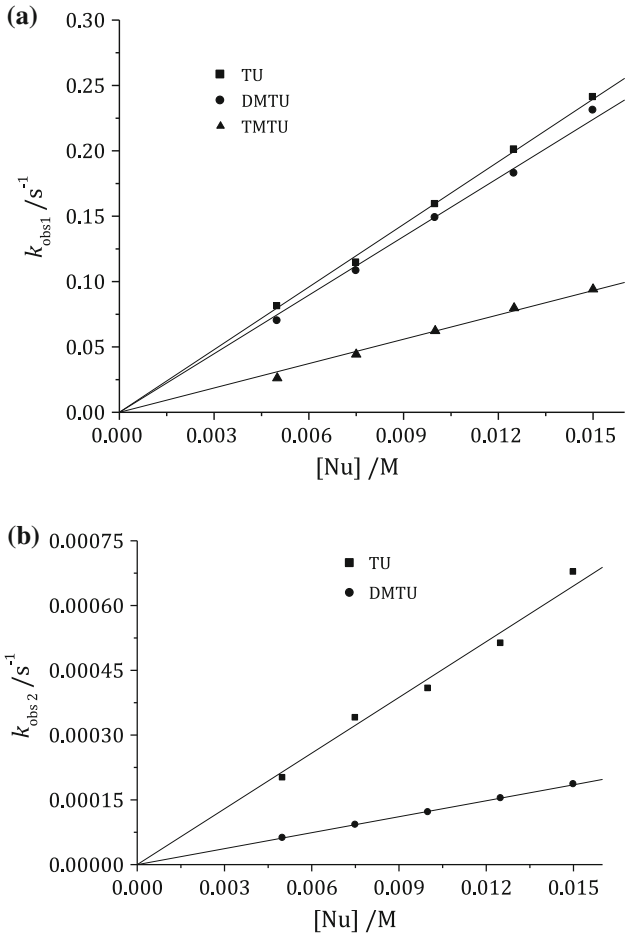


Fig. 5 Concentration dependence of $k_{obs1/2}$ for the substitution of aqua from **Ptdpha** (0.25 mM) by thiourea nucleophiles for (**a**) the first and (**b**) the second substitution steps at pH 2, $I = 0.1$ M $NaClO_4$ and 25 °C

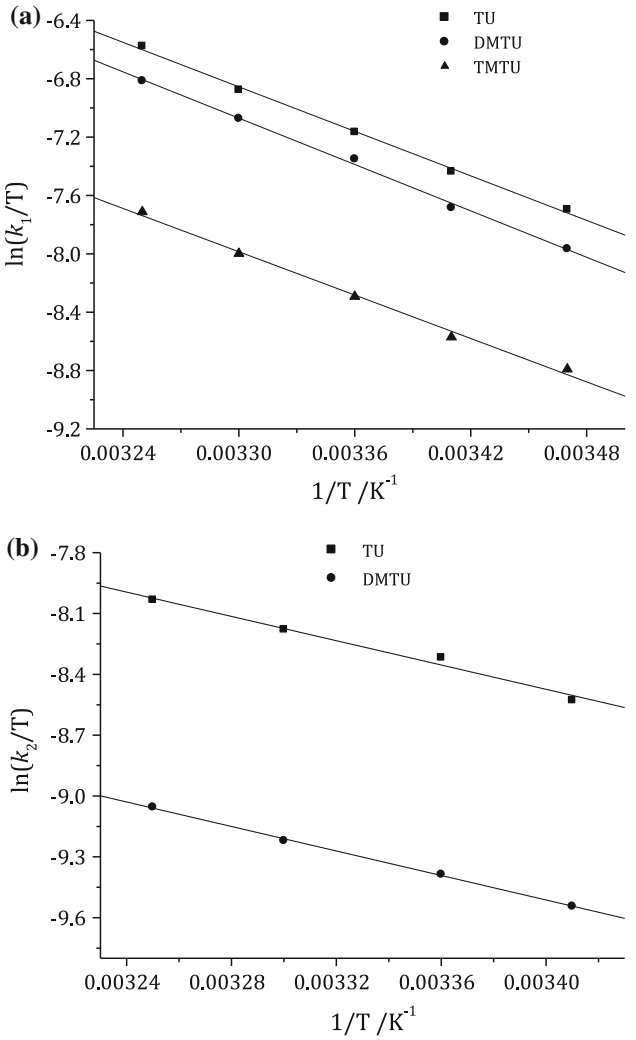


Fig. 6 Eyring plots for the determination of the thermal activation parameters for (**a**) the first and (**b**) the second substitution steps of 0.25 mM **Ptdppa** for the nucleophiles studied at pH 2 ($I = 0.1$ M $NaClO_4$)

increased on the ligand. For a series of Pt complexes, the resonance is shifted towards higher fields (more negative) when the donor atom varies from chlorine, nitrogen and sulphur in the following order: Cl < N < S. Platinum complexes have chemical shifts of $[PtN_3Cl]$ at $\delta = -1700$ to -2369 ppm [47, 48], $[PtN_2Cl_2]$ at $\delta = -1900$ to -2400 ppm [47], $[PtN_3S]$ at $\delta = -2800$ to -3200 ppm [48–50], $[PtN_2S_2]$ at $\delta = -3100$ to -3500 ppm [51–53] and $[PtS_4]$ at $\delta = -3800$ to -4800 ppm [47] whilst a value near $\delta = -5900$ ppm is indicative of five coordinated sulphurs [54]. The peak of the unreacted **Ptdppa–Cl$_2$** at $\delta = -2178.9$ and a new peak at $\delta = -3914.2$ ppm are therefore mainly due to $[PtN_2Cl_2]$ and $[PtS_4]$ before and after decoordination of dppa ligand, respectively. The assignment of these peaks in the ^{195}Pt NMR spectra to $[PtN_2Cl_2]$ and $[PtS_4]$ coordination spheres is in agreement with that reported in the literature [47, 54]. Furthermore, taking the solvent used into account, the chemical shifts of the aromatic protons in the spectrum resulting after addition of TU (excess) to the **Ptdppa–Cl$_2$** correspond well with those of the **dppa** free ligand (See Figure SI 26).

The ^{1}H NMR spectroscopy together with ^{195}Pt NMR results all support the proposed reaction Scheme 3. Therefore, it is reasonable to conclude that the presence of strong labilizing thiourea nucleophiles at the Pt(II) centre enhances ring opening of the bidentate ligand attached to the metal centre leading to metal–ligand dissociation upon exposure to excess TU. Results on ring opening influenced by the strong labilizing effect of thiourea nucleophiles have been reported by Jaganyi et al. [36, 55, 56].

Taking the simultaneous substitution reaction of the aqua ligands with TU as a reference, the rate constant of the complexes (Table 4) decreases in the order of $38.7 > 36.8 > 23.7 > 20.6 > 16.0$ M^{-1} s^{-1} for **Ptdpma**, **Ptdpea**, **Ptdppa**, **Ptdpba** and **Ptdpha**, respectively. The

Table 4 Summary of second-order rate constants and activation parameters for the first and second substitution steps

Complex	Nu	k_1 (M^{-1} s^{-1})	k_2 (M^{-1} s^{-1} × 10^{-2})	$\Delta H_1^{\#}$ (kJ mol^{-1})	$\Delta H_2^{\#}$ (kJ mol^{-1})	$\Delta S_1^{\#}$ (J K^{-1} mol^{-1})	$\Delta S_2^{\#}$ (J K^{-1} mol^{-1})
Ptdpma	TU	38.7 ± 0.6	106 ± 3	41 ± 0.5	27 ± 1	−115 ± 2	−193 ± 3
	DMTU	48.8 ± 0.5	2.4 ± 0.1	40 ± 0.5	36 ± 0.5	−115 ± 2	−114 ± 2
	TMTU	22.8 ± 0.4	–	40 ± 1	–	−122 ± 4	–
Ptdpea	TU	36.8 ± 0.7	8.6 ± 0.3	39 ± 2	37 ± 2	−133 ± 6	−127 ± 6
	DMTU	28.5 ± 0.6	2.2 ± 0.1	42 ± 1	46 ± 1	−122 ± 3	−121 ± 3
	TMTU	16.7 ± 0.2	–	38 ± 1	–	−142 ± 3	–
Ptdppa	TU	23.7 ± 0.3	7.4 ± 0.4	41 ± 1	24 ± 2	−119 ± 3	−185 ± 6
	DMTU	18.9 ± 0.4	1.4 ± 0.1	43 ± 1	25 ± 0.6	−115 ± 3	−191 ± 2
	TMTU	7.7 ± 0.1	–	40 ± 2	–	−132 ± 6	–
Ptdpba	TU	20.6 ± 0.3	5.0 ± 0.2	41 ± 2	40 ± 2	−121 ± 6	−125 ± 6
	DMTU	17.0 ± 0.1	1.2 ± 0.05	44 ± 1	37 ± 2	−113 ± 3	−196 ± 6
	TMTU	7.4 ± 0.2	–	39 ± 2	–	−137 ± 6	–
Ptdpha	TU	16.0 ± 0.1	4.3 ± 0.1	44 ± 1	22 ± 1	−113 ± 3	−157 ± 3
	DMTU	14.9 ± 0.2	0.7 ± 0.01	47 ± 0.4	39 ± 1	−105 ± 1	−169 ± 3
	TMTU	6.2 ± 0.1	–	79 ± 3	–	−120 ± 9	–
Pt(bpy)[a]	TU	5080 ± 275	1119 ± 22	45 ± 2	34 ± 2	−24 ± 7	−73 ± 5

[a] Data extracted from Ref. [22]

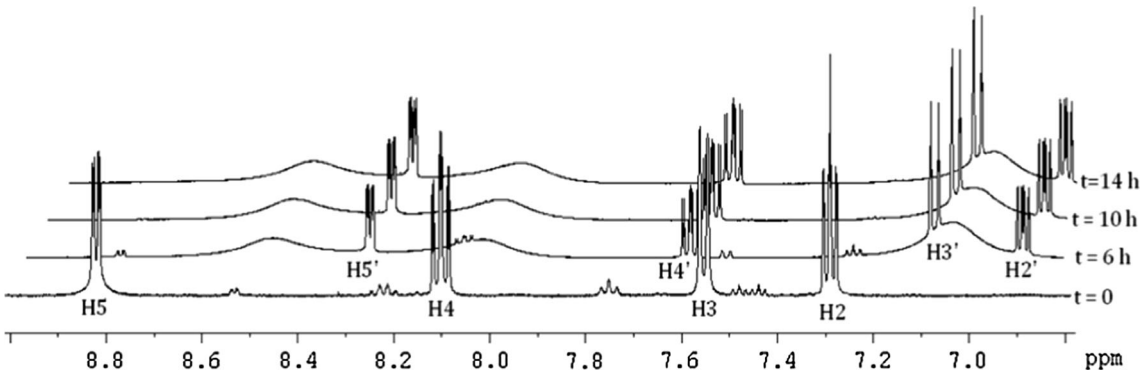
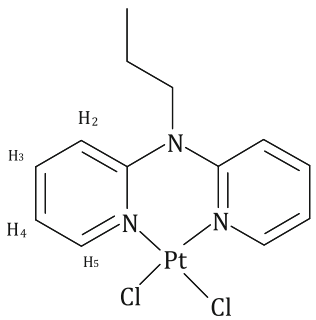


Fig. 7 ^{1}H NMR spectra of **Ptdppa–Cl_2** acquired during the reaction with TU 6 equiv. at the timescale shown on the spectra



Scheme 4 Numbering scheme employed for the pyridyl protons of **Ptdppa–Cl_2**

difference in reactivity can be ascribed to the steric hindrance and electronic effect of the pendant alkyl chain bonded on the tertiary nitrogen joining the *cis* pyridine rings. In all the five complexes, the pendant alkyl chain on the tertiary nitrogen is sticking out of the plane blocking the approach of the nucleophile from either the top or bottom of the square planar geometry depending on its length. In **Ptdpma** and **Ptdpea**, the chain is not long enough to block the entry of the nucleophile from both sides so the nucleophile can easily attack the Pt(II) centre from either side, resulting in higher rate of substitution reaction. However, for **Ptdppa**, **Ptdpba** and **Ptdpha** the aliphatic chain is bending downwards and so blocks the approach of the nucleophile from both sides of the square planar Pt(II), contributing to the lowering of reaction rate.

The individual HOMO and LUMO energies increase with an increase in alkyl chain length resulting in destabilization of the energies of both the HOMO and LUMO [57–59]. This affects electrophilicity of the complexes [60]

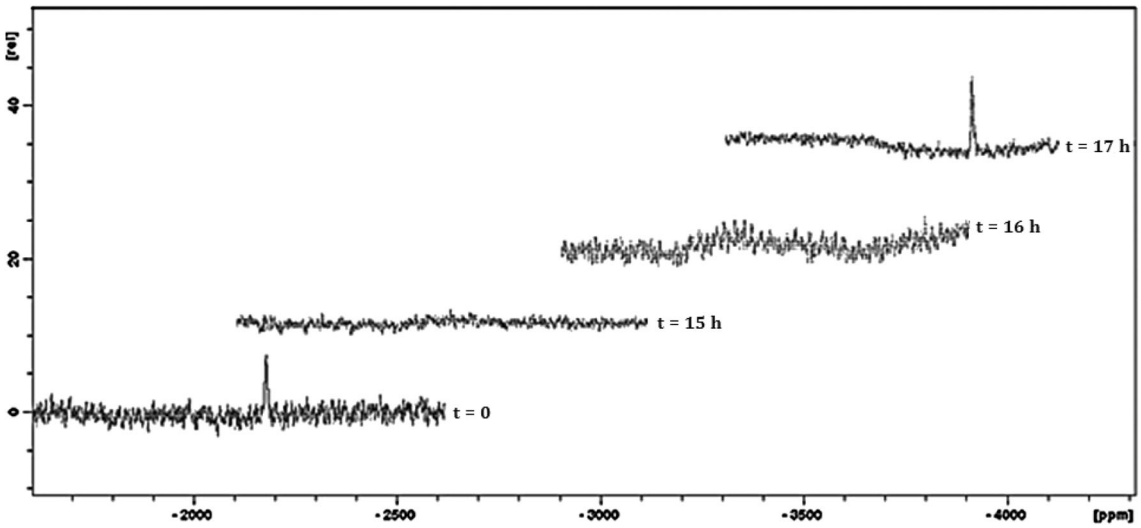


Fig. 8 ^{195}Pt NMR spectra of **Ptdppa–Cl$_2$** acquired during the reaction with TU (2 and 3 equiv.) in DMSO-d_6, at 30 °C

as shown in Table 3 such that the electrophilicity index decreases with an increase in σ-donicity of the aliphatic chain. The electronic effect of the alkyl chain to the tertiary nitrogen and to the pyridine nitrogens is supported by their dipole moments and NBO charges shown in Table 3. The tertiary nitrogen becomes more negative with an increase in alkyl chain length, as do the pyridine nitrogens. This causes the accumulation of the electron density into the LUMO type of the pyridyl rings making them weak π-acceptors, hence a less reactive Pt(II) centre towards substitution reaction. The decrease in reactivity of the complexes on moving from **Ptdpma** to **Ptdpha** in addition to the steric hindrance is also controlled by the σ-donation of electron density to the complex brought by the alkyl group through the tertiary nitrogen, which then destabilizes the transition state resulting in slow substitution reactions. The apparent increase in dipole moments by 1 debye with subsequent addition of –$(CH_2)_n$– fragment from **Ptdpma** to **Ptdpha** except from **Ptdppa** to **Ptdpba** where the increase is only 0.4 debye is expected given that the parameter correlates to the inductive negative charge in the complex [61].

A comparison also reveals that dpa Pt(II) complexes are generally less reactive towards thiourea nucleophiles by two orders of magnitude compared to bipyridine Pt(II) complex **Pt(bpy)** reported previously [22]. This is because dpa is a less π-acceptor ligand than bipyridine (bpy) [62, 63]. In addition, dpa coordinates with six-membered chelate rings instead of five-membered rings for bpy; thus, **Pt(bpy)** complex is rigid and planar with both pyridine moieties situated within the plane resulting in a very efficient π-back-donation of the incoming electron density from the nucleophile to the pyridine chelate [22]. This stabilizes the five-coordinate transition state relative to the ground state, since the ground state cannot benefit much from the π-back-donation given that the $6p_z$ orbital of the Pt centre is empty, leading to enhancement of the reaction rate. On the contrary, the bidentate chelate system in dpa Pt(II) complexes investigated in this study is more flexible adopting tilted pyridyl ring planes which then thwarts the flow of π-electrons around the ring, resulting in poor π-acceptor ability of the ligand and steric retardation on the metal centre towards the approach of the nucleophile.

The slower second substitution step can be ascribed to substitution of the labilized Pt-pyridinic N bonds in *trans* positions to two TU molecules, as a result of the strong *trans* effect of S-donor nucleophiles following their coordination to the soft Pt(II) centre. Having a closer look at this second substitution step, it is forty times slower than the first step in all the investigated complexes. The presence of the two thiourea ligands after the first substitution step makes the Pt(II) centre more crowded and sterically hindered. In addition, the σ-donation of the thiourea towards the Pt(II) centre makes it difficult for another nucleophile to attack. This accounts for the observed slow rate of reaction in comparison with the aqua substitution noting also that the leaving groups are different. This same reason explains why the second substitution reaction using the most sterically hindered tetramethyl thiourea (TMTU) nucleophile could not be followed.

Generally, the substitution of coordinated aqua ligands by the more sterically hindered nucleophiles DMTU and TMTU shows a clear dependence on the steric bulk of the nucleophiles [36, 55, 56, 64–66]. For example, the values of the rate constants for the first substitution step of **Ptdpea** decrease in the order TU (36.8) > DMTU (28.5) > TMTU (16.7). The most sterically hindered nucleophile TMTU shows the lowest reactivity reflecting the steric effects

characteristic of a mechanism involving bond making in the transition state. However, the first substitution step for **Ptdpma** shows that DMTU reacts faster than TU. This can be explained by the increase in basicity of its sulphur donor atom caused by the σ-donation of electrons by the two methyl groups relative to that of TU which outweighs any steric contribution [67].

For all investigated complexes, the enthalpies of activation ($\Delta H^{\#}$) are small and positive, whereas activation entropies ($\Delta S^{\#}$) are large and negative. This confirms the associative mode of activation for all investigated complexes and substitution steps [68].

Conclusion

The novel dpa Pt(II) complexes (**Ptdppa** and **Ptdpha**) and **Ptdpma**, **Ptdpea** and **Ptdpba** were synthesized, and the kinetics of ligand substitution with thiourea nucleophiles were studied. In all complexes, two substitution steps were observed corresponding to the simultaneous displacement of the aqua ligands and dechelation of the dpa ligand by thiourea nucleophiles. For both substitution steps, it was found that the reactivity of the metal centre decreases with the increase in length of aliphatic chain attached on the tertiary nitrogen bridging the *cis* coordinated pyridyl units. The trend in reactivity is attributed to the steric hindrance of the alkyl chain which blocks the attack of the nucleophile from either the top or bottom side of the Pt(II) centre.

In addition, the σ-donor effect of the pendant alkyl chain towards the tertiary bridging nitrogen is felt in the *cis* pyridine rings resulting in the decrease in their π-acceptor ability. The decrease in reactivity of the Pt(II) complexes with the increase in length of the alkyl chain is also supported by the dipole moments and the calculated electrophilicity indices. The decrease in enthalpy of activation ($\Delta H^{\#}$) with an increase in the reaction rate and the more negative entropy of activation ($\Delta S^{\#}$) is an indication of the low-energy transition state compared to the reactant state. These enthalpies and entropies of activation confirm an associative mode of activation common in many Pt(II) complexes.

Furthermore, the systematic tuning of the 2,2′-dipyridylalkylamine chelate ligands as shown in this work represents the possibility of having Pt(II) complexes with different steric and electronic behaviour which might improve the cellular activity of the Pt(II) compared to cisplatin through increased cellular uptake brought by the surfactant effect of the alkyl chain. A possible concern is the likelihood of disintegration of these complexes if used as drugs based on the evidence of dechelation of the ligand.

Acknowledgments The authors thank the University of Dar es Salaam (Tanzania) and University of KwaZulu–Natal (South Africa) for financial support to Grace Kinunda.

References

1. Bose D, Rahaman SH, Mostafa G, Walsh RDB, Zaworotko MJ, Ghosh BK (2004) Polyhedron 23:545
2. Rahaman SH, Bose D, Chowdhury H, Mostafa G, Fun H-K, Ghosh BK (2005) Polyhedron 24:1837
3. Camus A, Marsich N, Lanfredi AMM, Ugozzoli F, Massera C (2000) Inorg Chim Acta 309:1
4. Cotton FA, Daniels LM, Jordan GT, Murillo CA (1997) J Am Chem Soc 119:10377
5. Yang E-C, Cheng M-C, Tsai M-S, Peng S-M (1994) Chem Commun 20:2377
6. Youngme S, Chailuecha C, van Albada GA, Pakawatchai C, Chaichit N, Reedijk J (2005) Inorg Chim Acta 358:1068
7. Sletten J, Svardal K, Sørensen A (1993) Acta Chem Scand 47:1091
8. Paul AK, Mansuri-Torshizi H, Srivastava TS, Chavan SJ, Chitnis MP (1993) J Inorg Biochem 50:9
9. Yodoshi M, Okabe N (2008) Chem Pharm Bull 56:908
10. Fakih S, Tung WC, Eierhoff D, Mock C, Krebs B (2005) Z Anorg Allg Chem 631:1397
11. Grehl M, Krebs B (1994) Inorg Chem 33:3877
12. Puscasu I, Mock C, Rauterkus M, Röndigs A, Tallen G, Gangopadhyay S, Wolff JEA, Krebs B (2001) Z Anorg Allg Chem 627:1292
13. Bloemin MJ, Engelking H, Gütschow N, Karentzopoulos S, Krebs B, Reedijk J (1995) J Inorg Biochem 59:222
14. Rauterkus MJ, Fakih S, Mock C, Puscasu I, Krebs B (2003) Inorg Chim Acta 350:355
15. Mock C, Puscasu I, Rauterkus MJ, Tallen G, Wolff JEA, Krebs B (2001) Inorg Chim Acta 319:109
16. Bloemink MJ, Engelking H, Karentzopoulos S, Krebs B, Reedijk J (1996) Inorg Chem 35:619
17. Gangopadhyay SB, Röndigs A, Kangarloo SB, Krebs B, Wolff JEA (2001) Anticancer Res 21:2039
18. Tallen G, Mock C, Gangopadhyay SB, Kangarloo B, Krebs B, Wolff JEA (2000) Anticancer Res 20:445
19. Bogojeski J, Bugarčić ŽD, Puchta R, van Eldik R (2010) Eur J Inorg Chem 34:5439
20. Jovanović S, Petrović B, Čanović D, Bugarčić ŽD (2011) Int J Chem Kinet 43:99
21. Hochreuther S, Nandibewoor ST, Puchta R, van Eldik R (2012) Dalton Trans 41(2):512
22. Summa N, Schiessl W, Puchta R, van Eikema Hommes N, van Eldik R (2006) Inorg. Chem 45:2948
23. Soldatović T, Bugarčić ŽD, van Eldik R (2009) Dalton Trans 23:4526
24. Schreier S, Malheiros SVP, de Paula E (2000) Biochim Biophys Acta-Biomembr 1508:210
25. Murray SG, Hartley FR (1981) Chem Rev 81:365
26. Reedijk J (1999) Chem Rev 99:2499
27. Schiessl WC, Summa NK, Weber CF, Gubo S, Dücker-Benfer C, Puchta R, van Eikema Hommes NJR, van Eldik R (2005) Z Anorg Allg Chem 631:2812
28. Ashby MT (1990) Comments Inorg Chem 10:297
29. Origin7.5®™ SRO, v7.5714 (B5714), Origin Lab Corporation, Northampton, One, Northampton, MA, 01060, 2003
30. Frisch MJ, Trucks GW, Schlegel HB, Scuseria GE, Robb MA, Cheeseman JR, Scalmani G, Barone V, Mennucci B, Petersson GA, Nakatsuji H, Caricato M, Li X, Hratchian HP, Izmaylov AF, Bloino J, Zheng G, Sonnenberg JL, Hada M, Ehara M, Toyota K, Fukuda R, Hasegawa J, Ishida M, Nakajima T, Honda Y, Kitao O, Nakai H, Vreven T, Montgomery JA Jr., Peralta JE, Ogliaro F, Bearpark M, Heyd JJ, Brothers E, Kudin KN, Staroverov VN, Kobayashi R, Normand J, Raghavachari K, Rendell A, Burant JC,

Iyengar SS, Tomasi J, Cossi M, Rega N, Millam JM, Klene M, Knox JE, Cross JB, Bakken V, Adamo C, Jaramillo J, Gomperts R, Stratmann RE, Yazyev O, Austin AJ, Cammi R, Pomelli C, Ochterski JW, Martin RL, Morokuma K, Zakrzewski VG, Voth GA, Salvador P, Dannenberg JJ, Dapprich S, Daniels AD, Farkas O, Foresman JB, Ortiz JV, Cioslowski J, Fox DJ (2009) Revision A.1 Gaussian, Inc., Wallingford, CT. http://akira.ruc.dk/∼span get/help/g09/m_citation.htm
31. Becke AD (1997) J Chem Phys 107:8554
32. Lee C, Yang W, Parr GR (1988) Phys Rev B 37:785
33. Miehlich B, Savin A, Stoll H, Preuss H (1989) Chem Phys Lett 157:200
34. Hay PJ, Wadt WR (1985) J Chem Phys 82:299
35. Soldatović T, Jovanović S, Bugarčić ŽD, van Eldik R (2012) Dalton Trans 41(3):876
36. Mambanda A, Jaganyi D (2012) Dalton Trans 41:908
37. Hofmann A, van Eldik R (2003) Dalton Trans 15:2979
38. Hofmann A, Jaganyi D, Munro OQ, Liehr G, van Eldik R (2003) Inorg Chem 42:1688
39. Kumar L, Srivastava TS (1983) Inorg Chim Acta 80:47
40. Kidani Y, Asano Y, Noji M (1979) Chem Pharm Bull 27:2577
41. Dehand J, Jordanov J (1976) J Chem Soc Chem Comm 15:598
42. Howell BA, Walles E (1988) Inorg Chim Acta 142:185
43. Mebi CA (2011) J Chem Sci 123(5):727
44. Espenson JH (1995) Chemical kinetics and reaction mechanisms, 2nd edn. New York, McGraw-Hill
45. Eyring H (1935) J Chem Phys 3:107
46. Fazlur-Rahman AK, Verkade JG (1992) Inorg Chem 31:2064
47. Priqueler JRL, Butler IS, Rochon FD (2006) Appl Spectrosc Rev 41:185
48. Ma G, Min Y, Huang F, Jiang T, Liu Y (2010) Chem Commun (Camb) 46(37):6938
49. Crossley EL, Caiazza D, Rendina LM (2005) Dalton Trans 17:2825
50. Todd JA, Rendina LM (2002) Inorg Chem 41:3331
51. Norman RE, Ranford JD, Sadler PJ (1992) Inorg Chem 31:877
52. Todd JA, Caiazza D, Tiekink ERT, Rendina LM (2003) Inorg Chim Acta 352:208
53. Appleton TG, Connor JW, Hall JR, Prenzler PD (1989) Inorg Chem 28:2030
54. Grant GJ, Brandow CG, Galas DF, Davis JP, Pennington WT, Valente EJ, Zubkowski JD (2001) Polyhedron 20:3333
55. Jaganyi D, Ongoma P (2013) Dalton Trans 42:2724
56. Ertürk H, Puchta R, van Eldik R (2009) Eur J Inorg Chem 10:1331
57. Salzner U, Kızıltepe T (1999) J Org Chem 64:764
58. Kistler KA, Matsika S (2007) J Phys Chem A 111:8708
59. Mburu E, Matsika S (2008) J Phys Chem A 112:12485
60. Singh RK, Verma SK, Sharma PD (2011) Int J ChemTech Res 3(3):1571
61. Das M, Livingstone SE (1975) J Chem Soc Dalton Trans 452
62. Mittal SK, Kumar P, Ashok Kumar SK, Lindoy LF (2010) Int J Electrochem Sci 5:1984
63. Shepherd RE, Chen Y, Kortes RA, Ward MS (2000) Inorg Chim Acta 303:30
64. Jaganyi D, Ongoma P (2012) Dalton Trans 41:10724
65. Jaganyi D, Tiba F (2003) Transit Met Chem 28:803
66. Jaganyi D, Reddy D, Gertenbach JA, Mzunro OQ and van Eldik R (2004) Dalton Trans 299
67. Bruice PY (1998) Organic chemistry, 2nd edn. Prentice Hall, New York, pp 363–366
68. Tobe ML, Burgess J (1999) Inorganic reaction mechanisms. Addison-Wiley, Longman, Ltd.: Essex, 1999, pp. 30–33, 70–112